Geophys. J. R. astr. Soc. (1977) **49**, 59–85

Evidence for anisotropy in the upper mantle beneath Eurasia from the polarization of higher mode seismic surface waves

Stuart Crampin *Institute of Geological Sciences, Murchison House, West Mains Road, Edinburgh EH9 3LA*

David W. King* *NTNF/NORSAR, Kjeller, Norway*

Received 1976 July 2

Summary. Analysis of NORSAR records and a number of Soviet microfilms reveals second-mode surface waves propagating along paths covering a large part of Eurasia. These second modes in the 6–15-s period band are frequently disturbed by other surface-wave modes and by body-wave arrivals. However, in all cases, where the modes appear to be undisturbed and show normal dispersion, the Second Rayleigh modes have a slowly varying phase difference with the Second Love modes. This coupling has the particle motion of Inclined Rayleigh waves characteristic of surface-wave propagation in anisotropic media, where the anisotropy possesses a horizontal plane of symmetry. Numerical examination of surface wave propagating in Earth models, with an anisotropic layer in the upper mantle, demonstrate that comparatively small thicknesses of material with weak velocity anisotropy can produce large deviations in the polarizations of Inclined Rayleigh Second modes. In many structures, these inclinations are very sensitive to small changes in anisotropic orientation and to small changes in the surrounding isotropic structure. It is suggested that examination of second mode inclination anomalies of second mode surface waves may be a powerful technique for examining the detailed anisotropic structure of the upper mantle.

1 Introduction

All well-recorded wave trains of second-mode Rayleigh waves across Eurasia are accompanied by second-mode Love waves of comparable amplitude, although not usually having amplitude maxima at the same time on the seismogram. The wave trains show similar dispersion with a slowly varying phase difference between the Rayleigh and Love components. This coupling was first noticed by Crampin (1966a, 1967) and anisotropy in the upper mantle suggested as the cause. Support for this thesis has been difficult to find because of the rarity of good higher mode wave trains on recordings by conventional instrumentation in the period range (6–15 s) at which the higher modes sample the upper mantle. Fifteen

* Present address: Department of Geology and Geophysics, University of Sydney, New South Wales 2006.

years of conventional instrumentation in Eurasia have yielded a mere handful of well recorded higher modes. Processing digital recordings at NORSAR now greatly increases the number of higher mode wave trains available for study, and removes some of the uncertainties of digitized photographic seismograms.

The application of simple bandpass filtering techniques, to a number of Eurasian events recorded on the long period array at NORSAR, reveals well-recorded higher mode wave trains, arriving from a 100° azimuth range, displaying sagittal/transverse coupling for all paths over homogeneous continental structure. In this paper, we shall present higher mode polarizations at NORSAR and at a number of conventional stations, for a network of paths covering a large part of Eurasia and demonstrate that, for much of their wave trains, the Second Rayleigh and Love modes are coupled together in a polarization characteristic of anisotropy in the upper mantle.

For convenience in discussing the observations, we shall speak of the coupling of the familiar Second Rayleigh (2R) and Second Love (2L) modes, and later compare the observed polarizations with those calculated for Generalized modes propagating in Earth models containing anisotropy.

2 Higher mode propagation in Eurasia

The propagation of higher mode surface waves requires comparatively uniform crustal and upper mantle structure. The graver modes, 2R and 2L in the 6–15-s band, have a large proportion of their energy travelling in the top few kilometres of the upper mantle, and are consequently very sensitive to variations in the structure near the Moho. In particular, higher modes are rapidly attenuated in regions of structural change, such as mountain roots, and oceanic–continental margins. Eurasia provides the largest existing homogeneous area for the propagation of continental higher modes, and 2R and 2L have been observed (Crampin 1964a) for many paths within the area bounded to the west and south by the Scandinavian, Alpine, and Himalayan mountain systems, and to the north and east by the 1000-m depth line in the Arctic Ocean and the inner seas of the Pacific island arc structures. However, well-recorded wave trains of higher modes are scarce even along suitable paths as they appear on an active part of the seismogram between the *S* phase and the fundamental-mode surface waves, where there are many disturbing arrivals. Frequently, several higher modes are generated by the same event, and form interfering wave trains, which are difficult to separate. The beginning of the higher modes may be disturbed by the *S* coda. The *S* and multiple *S* phases may be followed, at some epicentral distances, by shear-coupled *PL* waves and shear-coupled higher modes, which interfere with the direct higher modes. The end of the higher mode wave trains is usually hidden in the fundamental Rayleigh (FR) and Love (FL) modes. Multipathing is probably not a serious difficulty with higher modes as they are likely to be severely attenuated by any phenomena causing multipathing.

Thus, undisturbed higher mode wave trains require the source to be of suitable depth and focal mechanism to excite a single mode along a suitable path, but not excite significant body-wave arrivals in the particular distance range. With all these disturbing signals, recordings from conventional instrumentation of fixed magnification seldom show good higher mode wave trains for more than a limited distance range, even from events which generate large-amplitude higher modes. Photographic records have to be digitized manually, and for reliable higher modes to be extracted, the higher modes must be clearly visible above the disturbing signals, and this is seldom the case. Digital recordings have the advantage that the higher modes often have sufficient frequency separation from the disturbing signals to be extracted by simple filtering techniques.

Some of the difficulties associated with higher mode excitation and propagation are exemplified by the 630817 earthquake in the Ryukyu Islands (Table 1), which generated 2R and 2L along many paths across Eurasia (Crampin 1966a). The UPP seismogram – Fig. 3(a) – is one of the longest continuous wave trains of higher modes (nearly 60 cycles) yet recorded. These higher modes propagated through a narrow window in the East China Sea which permits the passage of continental higher modes. This appears to be the only window permitting higher modes to propagate across Asia from island arc earthquakes in the Western Pacific. Since 1963, there have been a number of events with apparently similar focal parameters in the Ryukyu Islands, yet none has produced higher mode records of comparable amplitude or duration, even on filtered NORSAR records.

The dispersion of 2R and 2L along homogeneous continental paths in Eurasia has been regionalized by Crampin (1966a). The period of a higher mode in such uniform structures, at any given group or phase velocity, is approximately proportional to the depth to the Moho, which is the most significant interface influencing the dispersion of 2R and 2L. The period would be strictly proportional if all the dimensions scaled in the same way. Thus second modes at any given period propagate at different velocities depending on the thickness of the crust along the path. This makes it difficult to combine, into one analysis scheme, second mode wave trains at different stations and from different paths to the same station, and is one of the contributing causes to the wide variation in the behaviour of the second modes along different paths.

3 Observations

The higher mode paths we examine are for a range of azimuths to NORSAR, and a range of azimuths from two earthquakes. They are mapped in Fig. 1 and listed in Table 1. The NORSAR records are, with one exception, taken from LP site No. 11 on the north-eastern edge of the array. The three component records are processed, by a 6–18-s bandpass filter without phase-shifts, with the intention of separating the second modes. Complete separation would require adaptive filtering techniques, which have not been attempted because of the danger of contaminating the polarizations by introducing ill-controlled phase shifts into the traces. The pass band of the filter has been kept as wide as possible for the same reason. This has meant that the filtered traces may contain sections of wave trains from higher modes other than the second, and is one further contributing cause of the irregularities which are displayed.

The filtered traces are rotated parallel and perpendicular to the great circle direction, and lines are drawn through the rotated traces at peaks of the wave trains on the vertical component. These striped sections of the records are between group arrivals of 4.4 and 3.2 km/s, unless otherwise indicated, and include all the second mode wave trains in the pass band of interest. The wave train within the striped section, which shows normally dispersed second-mode wave trains, has been underlined. Confirmation that the underlined sections are of second modes is given by the dispersion of the Ryukyu Islands–UPP path in Fig. 2, obtained by the Time Series Analysis Program of Burton & Blamey (1972). The turning points at the low velocity end of the dispersion curve in this figure are probably due to the presence of modes higher than the second. The dispersion of the second modes along this path, and of the underlined sections of all the records is typical of propagation across Eurasia (Crampin 1966a).

3.1 POLARIZATION DIAGRAMS

The motion of the horizontal components and the phase relationship with the vertical is demonstrated by polarization diagrams for successive 15-s windows of the underlined traces.

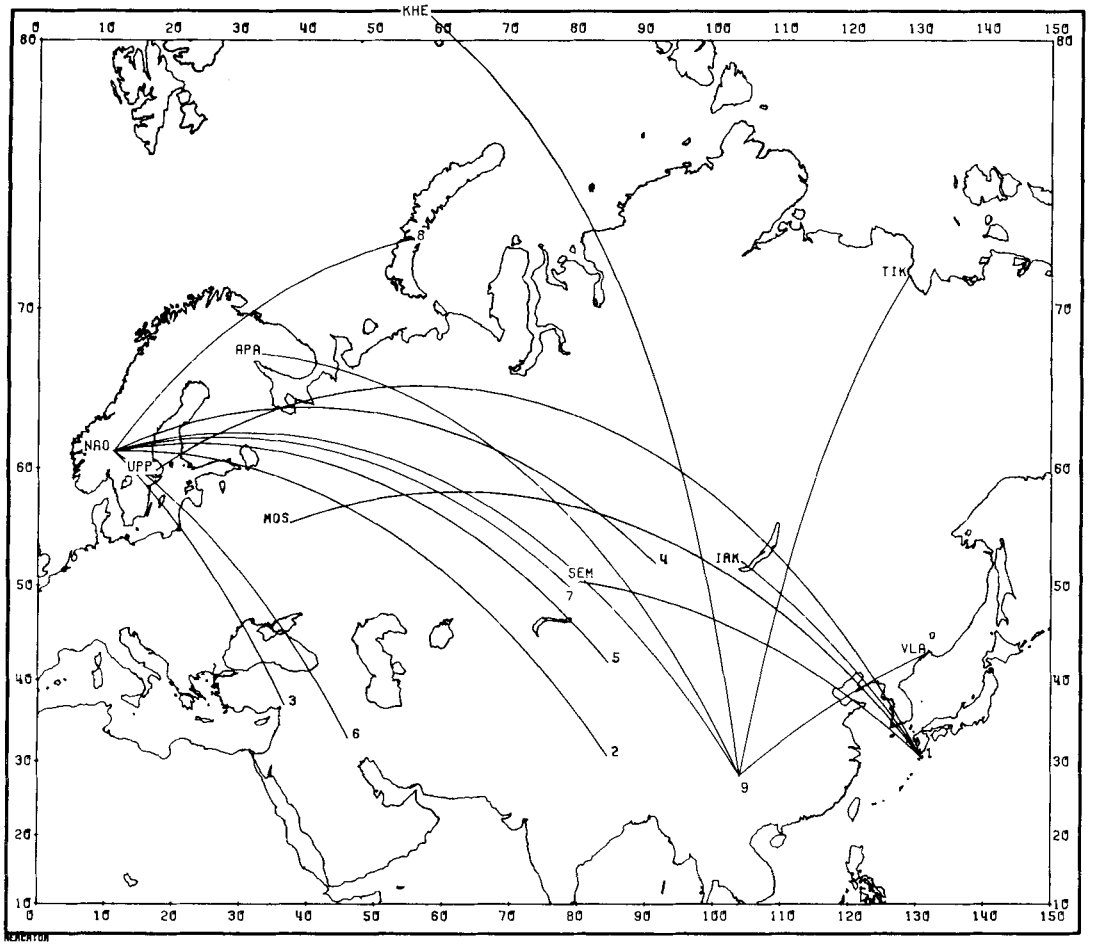

Figure 1. Great circle paths for events listed in Table 1.

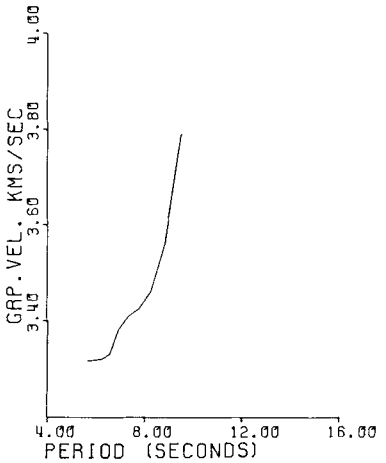

Figure 2. Group velocity of the vertical component for the Event 1 Ryukyu Islands to UPP path. (Seismogram in Fig. 3(a).)

Table 1. Higher mode paths.

Figures	Station	Event	y m d	h m s	Lat (N)	Long (E)	Depth (km)	m_b
3(a), 4(a)	UPP							
3(b), 4(b)	IRK	(1) Ryukyu Islands	63 08 17	11 12 41.2	30.6	130.9	27	6.8
3(c), 4(c)	MOS							
3(d), 4(d)	SEM							
7(b), 8(b)	NAO11	(2) Tibet	71 05 03	00 33 24.6	30.8	84.3	27	5.3
7(d), 8(d)	NAO11	(3) Turkey	71 08 17	04 29 33.4	37.1	36.8	35	5.0
5(b), 6(b)	NAO11	(4) Central Russia	71 08 24	16 33 21	52.2	91.6	12	5.4
7(a), 8(a)	NAO11	(5) Northern Sinkiang Province	72 04 09	04 10 48.9	42.1	84.6	21	5.8
7(c), 8(c)	NAO12	(6) Iran/Iraq Border	72 06 13	00 55 38.0	33.1	46.2	31	5.0
5(d), 6(d)	NAO11	(7) Eastern Kazakhstan explosion	73 07 23	01 22 57.7	49.9	78.8	0	6.1
5(a), 6(a)	NAO11	(8) Novaya Zemlya explosion	73 09 12	06 59 54.6	73.3	55.0	0	6.8
5(c), 6(c)	NAO11							
9(a), 10(a)	APA							
9(b), 10(b)	KHE	(9) Szechwan Province	74 05 10	19 25 15	28.2	104.0	11	6.2
9(c), 10(c)	TIK							
9(d), 10(d)	VLA							

The polarization diagrams show two cross-sections of the particle motion: a vertical section through the great circle (a *sagittal* section) with directions towards (T) and away (A) from the source indicated, and a horizontal section with the great circle indicated. Each cross-section is separately normalized – the largest relative amplitude being shown at the bottom right-hand side.

The four seismograms in Fig. 3 show second modes at different distances within a narrow azimuth range from Event 1. The wave train of the underlined traces is mainly on the vertical and transverse. As noted above, the 1-UPP path is almost the longest homogeneous continental path along which higher modes can be expected to propagate. This record has been much investigated (Crampin 1964b, 1966a, etc.), and shows many typical features of higher mode propagation. The higher modes cannot be completely separated by a single bandpass filter. Consequently, the beginnings of the striped sections of the seismograms usually show frequencies from some higher order modes, and the later sections again show fragments of higher order modes (as was suggested by the dispersion curve in Fig. 2). Certainly, almost all continental higher modes possess some irregularity. The polarization diagrams in Fig. 4 show many irregularities, but the predominant motion is approximately linear in the horizontal plane and elliptical in the vertical plane (the motion in the sagittal section frequently appears as a vertical line because the plane of motion is often perpendicular to the sagittal cross-section). This characteristic pattern alternates with short sections where the motion is elliptical in three dimensions and usually very irregular.

Seismograms in Figs 5 and 7 show higher modes arriving at NORSAR from 100° of azimuth ranging from Novaya Zemlya in the North to Turkey in the South. The paths from Novaya Zemlya and Sinkiang Province have been recognized previously as transmitting large amplitude higher modes to Scandinavia (Crampin 1966b, 1964b). All the polarization diagrams in Figs 6 and 8 have their predominant motion in the same characteristic pattern as in Fig. 4.

The seismograms in Fig. 9 show second modes propagating from Event 9 for a range of paths and directions not otherwise represented in Fig. 1. There are few seismic stations in northern USSR, and it is difficult to find suitable seismograms from earthquakes generating large amplitude higher modes. Consequently, there is little choice of seismogram and the second modes in Fig. 9 are poorly recorded compared with those in the previous figures. Nevertheless, despite the small-amplitude signals, all the polarization diagrams in Fig. 10 have their predominant motion in the same characteristic pattern.

The wave trains show many irregularities, but examination of the underlined seismograms in Figs 3, 5, 7 and 9 shows that the vertical and transverse components show essentially the same dispersion often with cycle by cycle correlation – with rotated horizontal components having a slowly varying phase difference of about $\pi/4$ with the vertical component. Examination of the corresponding polarization diagrams shows the predominant motion on the horizontal sections is almost linear, often nearly perpendicular to the great circle. On the sagittal section the motion is largely elliptical with very little radial component. This characteristic pattern describes elliptical motion in a vertical plane inclined to the direction of propagation, and is the *Inclined Rayleigh* motion recognized by Crampin (1975) as characteristic of propagation in anisotropic structures, where the anisotropy possesses a horizontal plane of symmetry.

Assuming isotropic Earth structure, this observed polarization behaviour could be explained in one of two ways: either (1) the second modes 2R and 2L are decoupled, but possess identical dispersion, or (2) the 2R has larger amplitude than 2L and arrives from approximately 90° off the great circle. Both hypotheses are untenable:

(1) Two decoupled waves such as 2R and 2L are most unlikely to possess identical dispersion

over the length and breadth of Eurasia where this motion has been observed (Fig. 1), and react in exactly the same way to any, albeit minor, structural irregularities along the path.
(2) (a) Higher modes are very sensitive to structural inhomogeneities, and are most unlikely to survive such severe refraction or reflection.

(b) It is improbable that any combination of inhomogeneities could produce such severe refraction to all stations along particular paths (Fig. 3 shows seismograms at various distances from Event 1), and for all azimuths of arrival at a single station (Figs 5 and 7 show seismograms at range of azimuths to NORSAR).

3.2 ARRAY ANALYSIS

There is considerable variation of the second modes for each event as they progress across NORSAR, probably associated with crustal thickening of the underlying structure. This lack of coherency is to be expected for comparatively short-period surface waves (Mack 1972), and prohibits any attempt to find an average polarization across the array. Signals arriving from the east, perpendicular to the strike of the Scandinavian mountains at the latitude of NORSAR, show least variation. In view of the tendency of Rayleigh waves, at least for the fundamental mode, to multipath (Capon 1970), it is important to establish that the polarization of the second modes is not caused by arrivals off great circle directions.

High resolution (HR) frequency-wave number spectra described by Capon (1969) was used to estimate phase velocity and azimuth of phase arrival for segments of wave trains at specified frequencies. Event 5 has the most coherent second-mode wave train crossing NORSAR from a great circle direction of 78°. High-resolution f–k spectra for the Fundamental Rayleigh, Fundamental Love, and Second mode (vertical component) for this event are shown in Fig. 11. Application of HR is sensitive to the setting-up parameters. However, the three spectra appear to be excellent determinations, with satisfactory power peaking. The 20-s Fundamental Rayleigh mode phase arrives almost exactly along the great circle. The 20-s fundamental Love mode arrives 5° to the north, and the 15-s second mode arrives 10° to the south of the great circle. It is difficult to make a realistic estimate of the accuracy or significance of these deviations; certainly the velocity determinations for the Fundamental Love and Second modes are high, probably due to the changing structure, but the azimuth deviations are comparatively small for all the modes, and clearly the 80° or 90° inclinations of the second-mode polarizations for this event – Fig. 8(a) – cannot be attributed to off great circle arrivals. The HR spectra for second modes from other events in Table 2 were of much lower quality, but all were consistent with arrivals within a few degrees of the great circle.

An attempt was made to determine the azimuth of the group velocity arrival. The technique of using narrow bandpass filters to estimate the arrival of the energy at a given period (Dziewonski, Bloch & Landisman 1969) was applied to the second modes on the vertical components at each of the LP sites, and the azimuth and velocity across the array obtained by combining the energy arrivals from all the sites. Although the solution appears stable the resolution is poor, mainly because of the small aperture of the array in relation to the wavelength of the group velocity envelopes. No events produced reliable estimates of second-mode energy arrivals, but, within the expected resolution, all solutions were compatible with the true arrival being within a few degrees of the great circle.

In addition to the above arguments, it is worth remarking that all well-developed higher mode wave trains across Eurasia show this characteristic pattern of polarization, and that the sections of the higher mode wave trains showing this pattern most clearly are, in all cases, those with largest amplitude and with most regular dispersion. This suggests that the

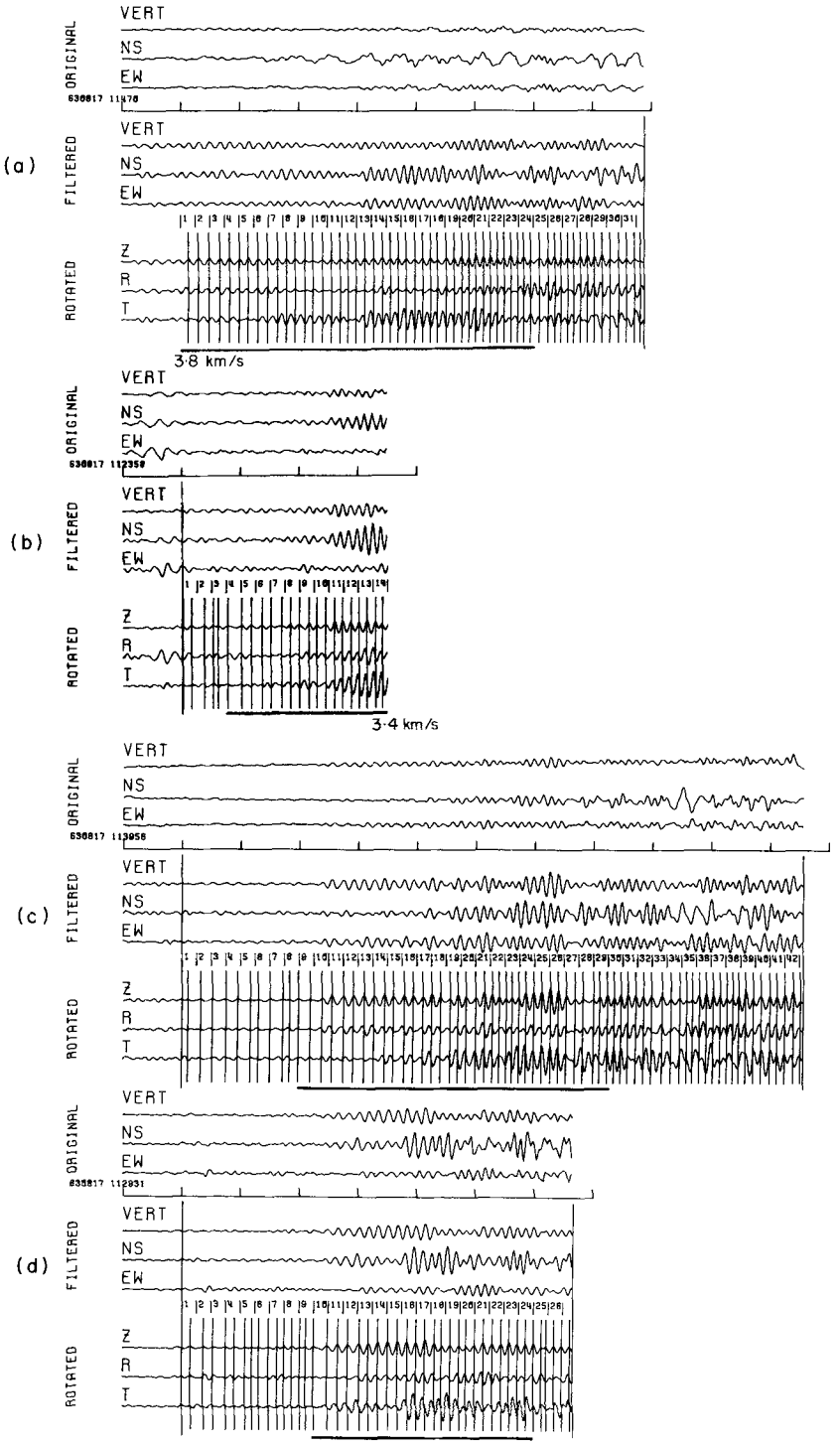

Figure 3. Original three-component seismograms, filtered, and rotated radially (R) and transverse (T) to the great circle. (a) Event 1 Ryukyu Islands to UPP, (b) Event 1 Ryukyu Islands to IRK, (c) Event 1 Ryukyu Islands to MOS, (d) Event 1 Ryukyu Islands to SEM.

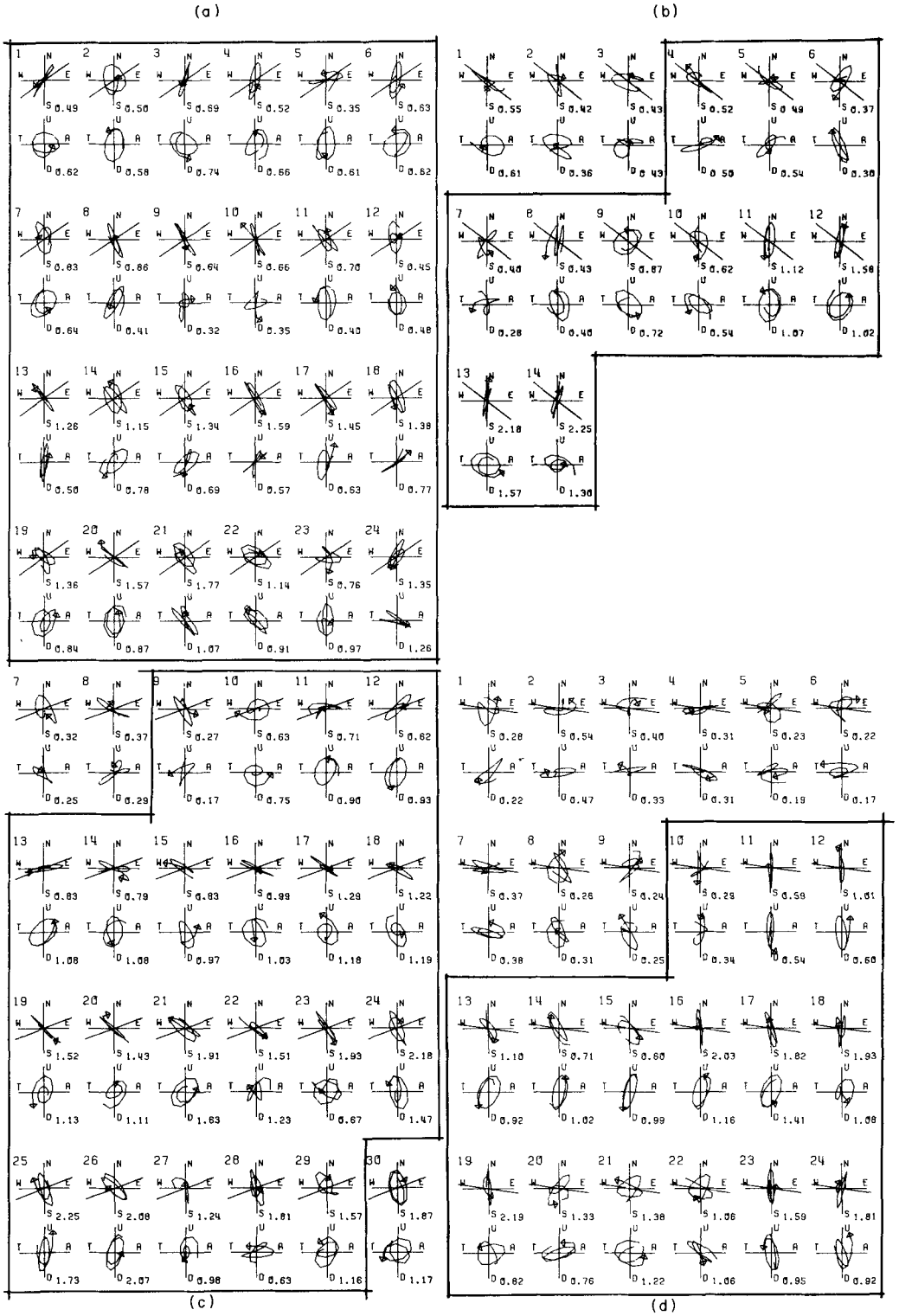

Figure 4. Polarization diagrams for successive 15-s intervals of the four seismograms in Fig. 3, respectively. The identification number of each pair of diagrams refers to the identification number of the time-window on the seismograms. The outlined diagrams refer to the underlined sections of the seismograms showing normally dispersed, second-mode wave trains.

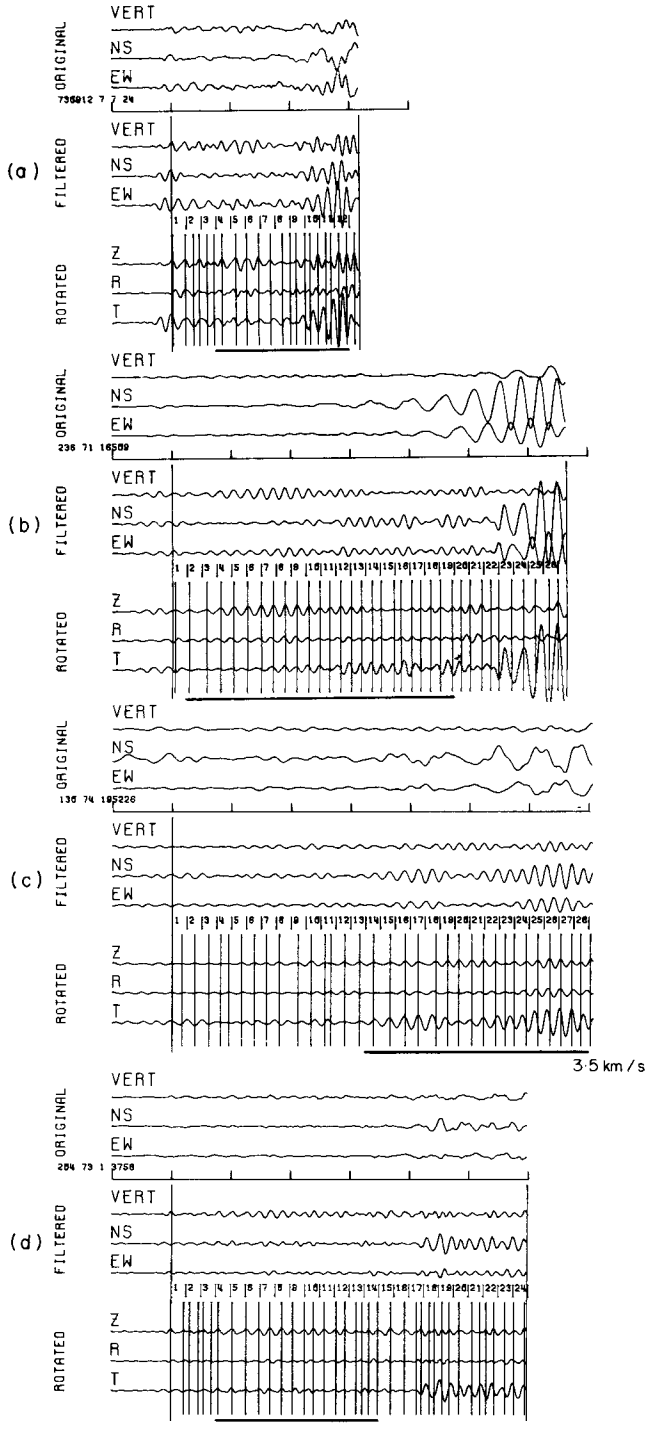

Figure 5. NORSAR seismograms: (a) Event 8 Novaya Zemlya to NAO11, (b) Event 4 Central Russia to NAO11, (c) Event 9 Szechwan Province to NAO11, (d) Event 7 Eastern Kazakhstan to NAO11.

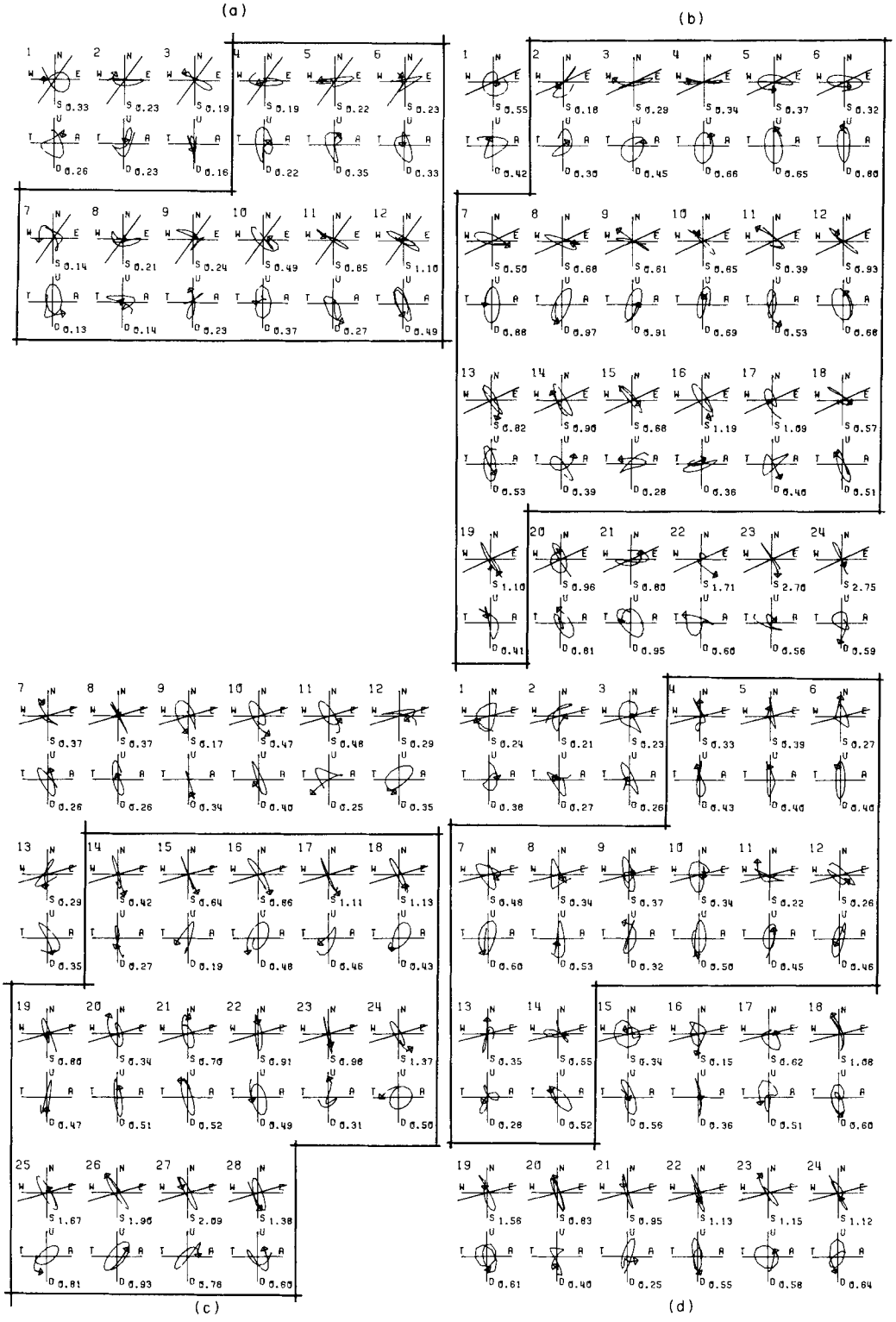

Figure 6. Polarization diagrams for seismograms in Fig. 5.

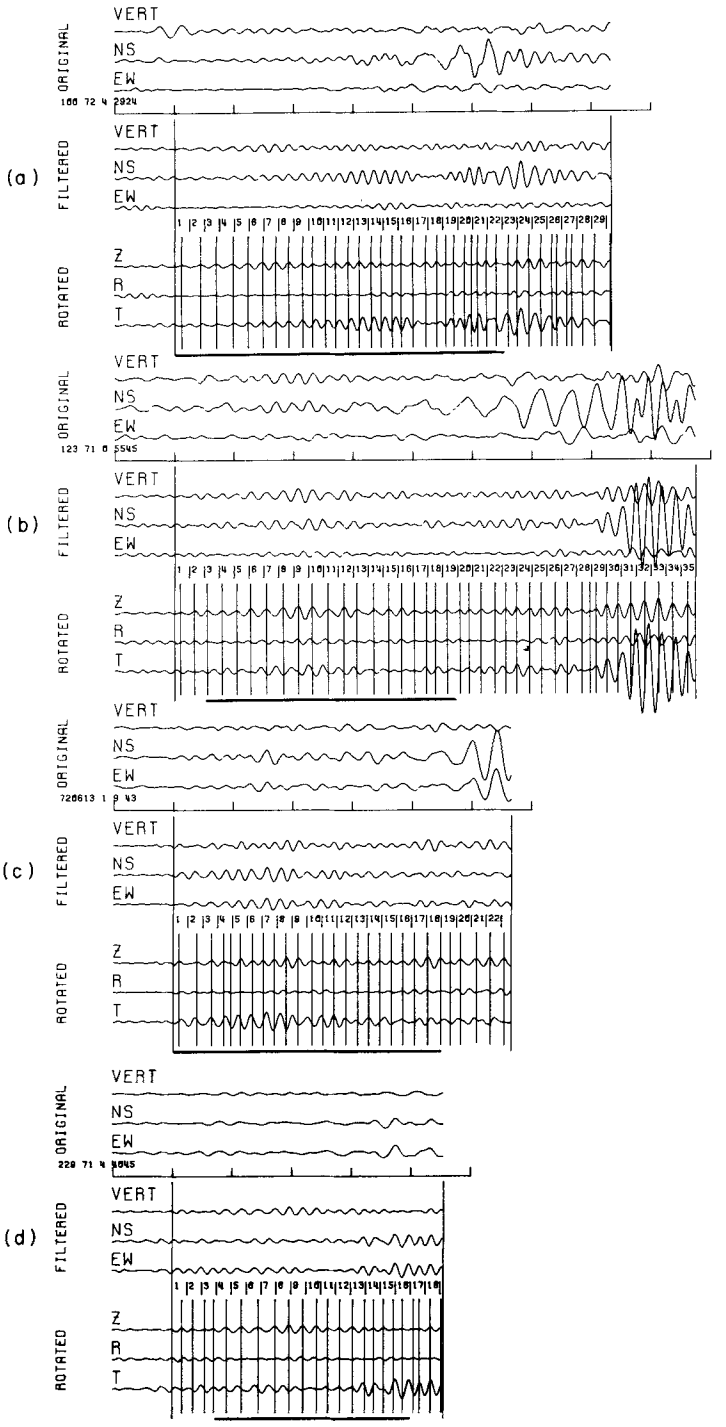

Figure 7. NORSAR seismograms: (a) Event 5 Northern Sinkiang Province to NAO11, (b) Event 2 Tibet to NAO11, (c) Event 3 Iran/Iraq Border to NAO12, (d) Event 3 Turkey to NAO11.

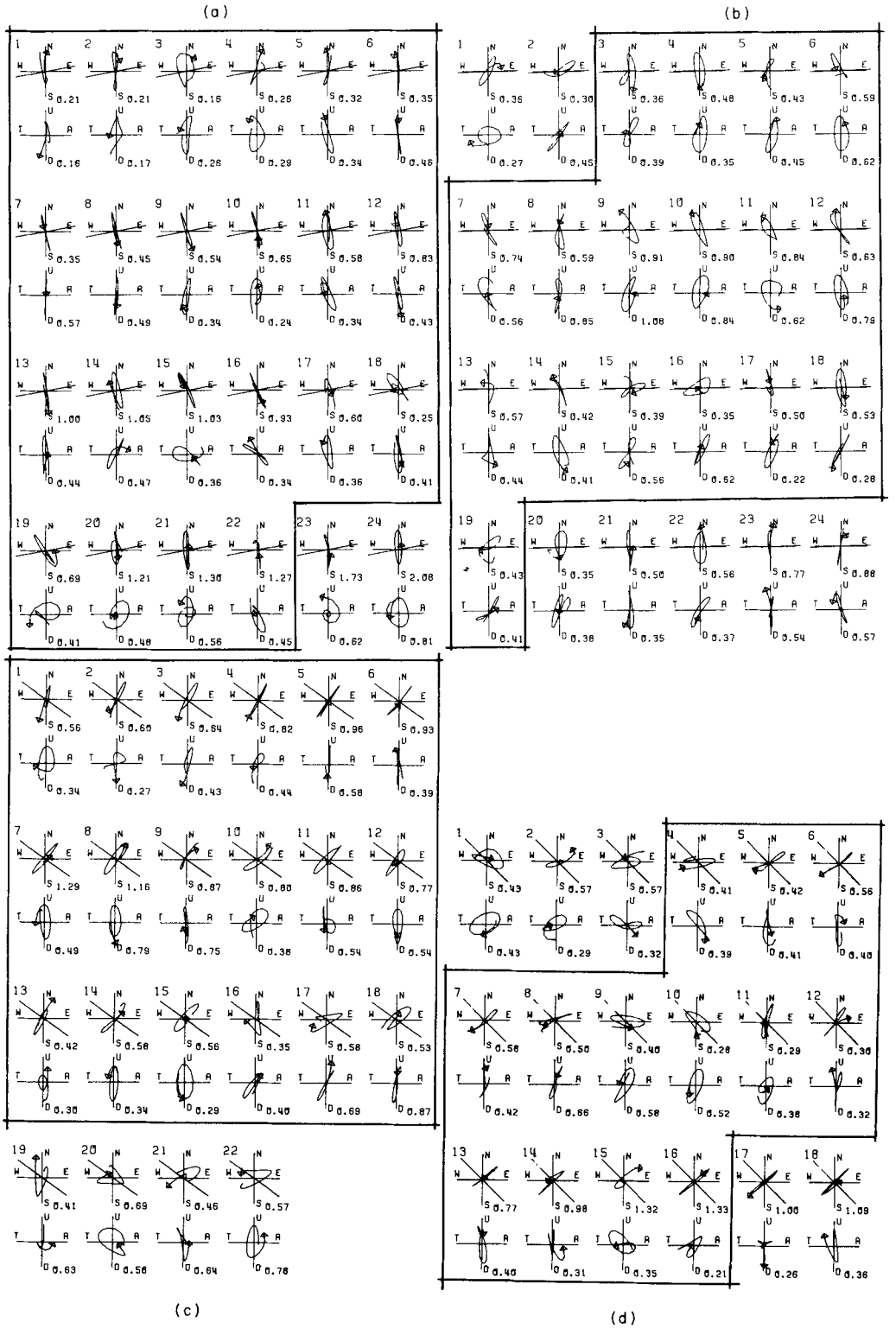

Figure 8. Polarization diagrams for seismograms in Fig. 7.

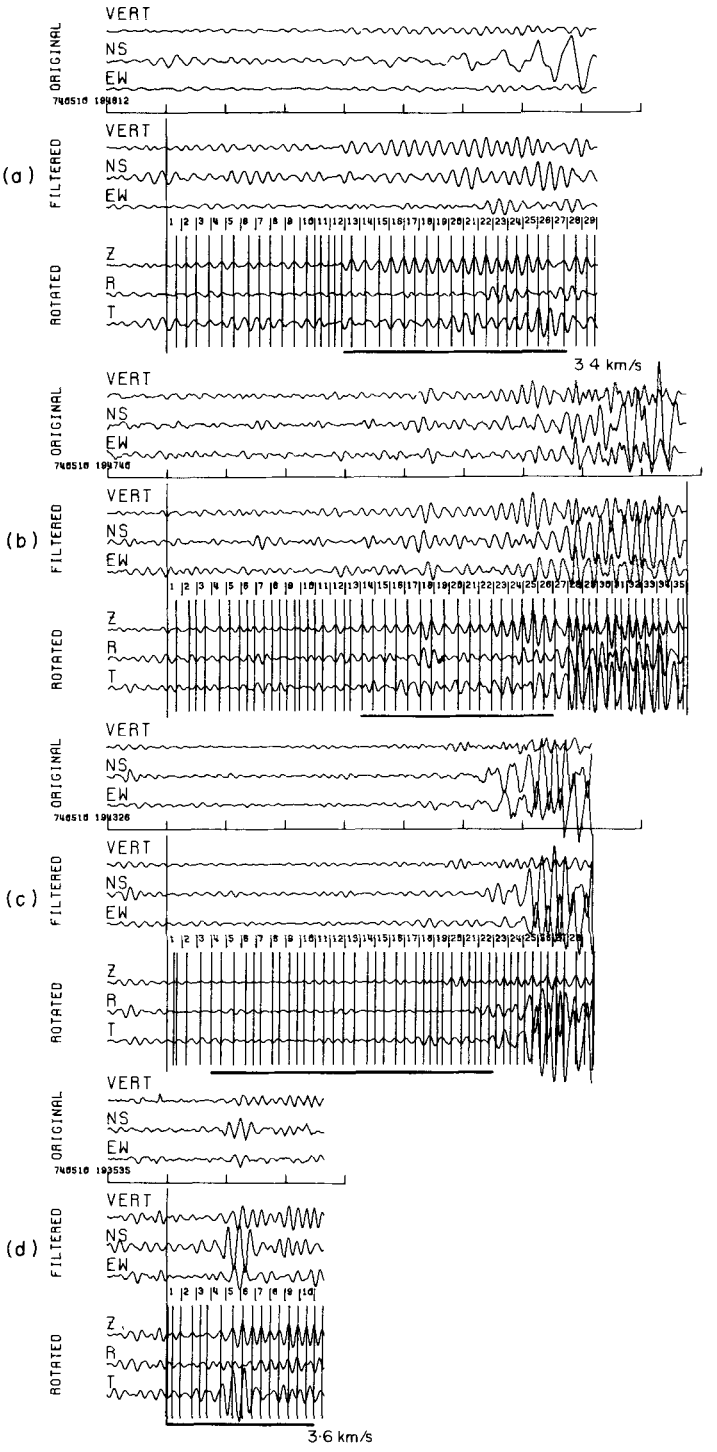

Figure 9. Seismograms: (a) Event 9 Szechwan Province to APA, (b) Event 9 Szechwan Province to KHE, (c) Event 9 Szechwan Province to TIK, (d) Event 9 Szechwan Province to VLA.

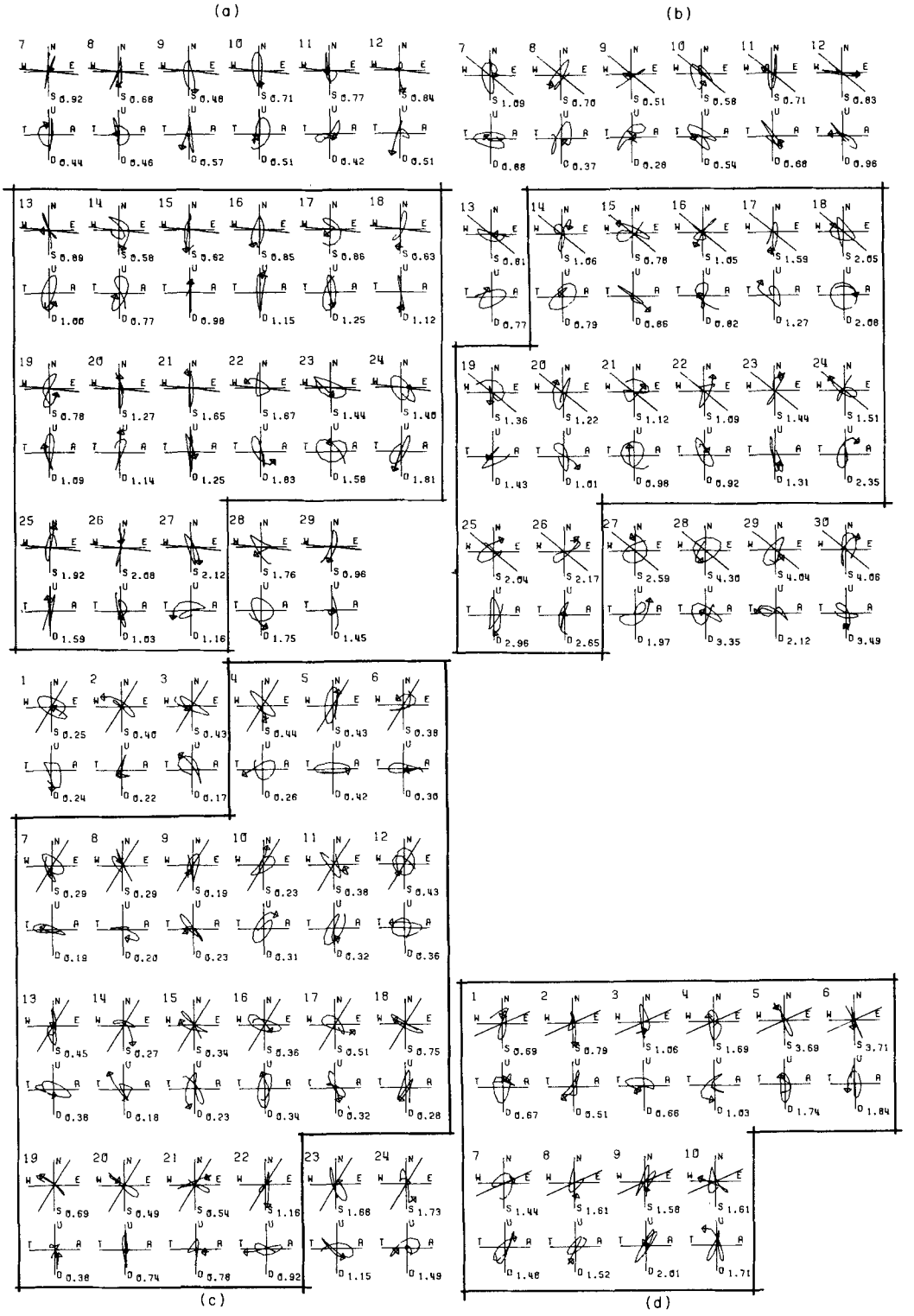

Figure 10. Polarization diagrams for seismograms in Fig. 9.

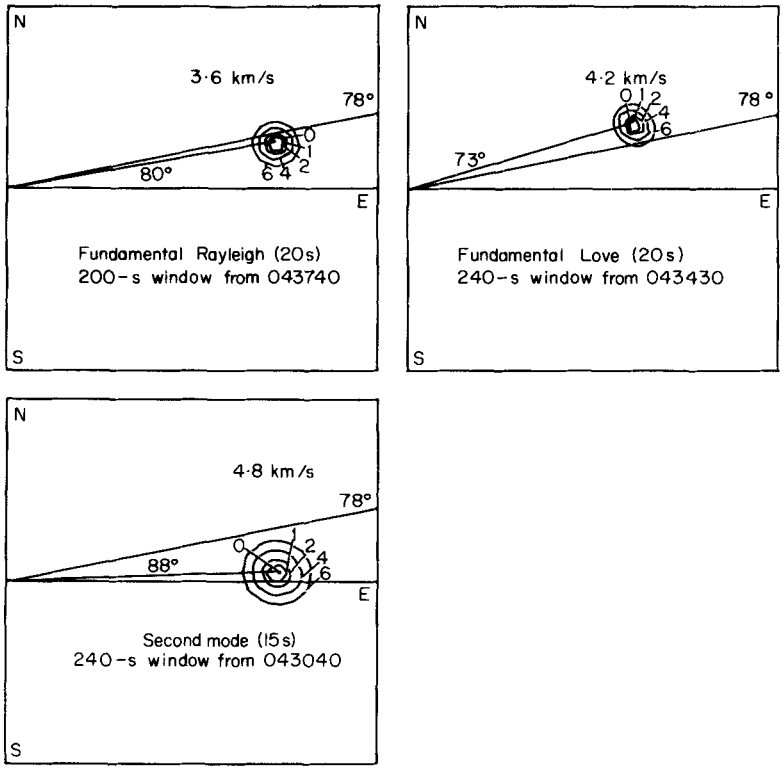

Figure 11. Direction and phase velocity arrivals at NORSAR from Event 5 determined by high-resolution frequency-wave number spectra.

pattern is characteristic of well-developed second-mode wave trains, and that departures from the pattern are due to irregularities of structure, rather than the characteristic patterns themselves being due to the coincidence of two decoupled modes.

We conclude that the characteristic patterns of particle motion cannot be easily interpreted in terms of isotropic structures. Sagittal and transverse components can only be coupled if there is some azimuthal variation of properties, that is some form of anisotropy in the structures penetrated by the second modes. We shall interpret the observations in terms of elastic anisotropy, for which we are able to calculate the propagation and show that such anisotropy within the upper mantle would produce similar effects to those observed.

4 Surface waves in anisotropic media

A matrix formulation for the calculation of dispersion characteristics of surface waves in layered anisotropic media was developed by Crampin (1970), and programmed by Crampin & Taylor (1971). They showed that surface waves propagate in anisotropic structure as one family of Generalized modes with coupling between the sagittal and transverse motion. In many structures, where the anisotropy is weak (either due to the thinness of the layer or to the small variation of properties with direction), many of the characteristics of Generalized modes are equivalent to alternate Rayleigh and Love modes. In such structures, the Generalized modes FG, 2G, 3G and 4G are approximately equivalent in dispersion and polarization to the isotropic Fundamental Rayleigh, Fundamental Love, Second Rayleigh and

Table 2. Equivalent notations for well separated normal mode surface waves in anisotropic and isotropic structures.

Generic names sometimes adopted in this paper	Mode nomenclature in structures containing anisotropy		Mode nomenclature in isotropic structures		
	Name	Abbrev.	Name	*Classification	Abbrev.
First modes	Fundamental Generalized	FG	Fundamental Rayleigh, First symmetric Rayleigh	M_{11}	FR
	Second Generalized	2G	Fundamental Love	–	FL
Second modes	Third Generalized	3G	Second Rayleigh, First asymmetrical Rayleigh, First higher Rayleigh, First shear	M_{21}	2R, 2nd R
	Fourth Generalized	4G	Second Love, First higher Love	–	2L, 2nd L
Third modes	Fifth Generalized	5G	Third Rayleigh, Second symmetric Rayleigh, Second higher Rayleigh, Second shear	M_{12}	3R, 3rd R
	Sixth Generalized	6G	Third Love, Second higher Love	–	3L, 3rd L

In this paper the collective name higher modes is sometimes used for unspecified second and third modes.
* The classification is that adopted by Tolstoy & Usdin (1953).

Second Love modes, respectively. The approximate relation between Generalized modes and isotropic modes are given in Table 2.

There are three ways in which the presence of anisotropy in the upper mantle affects surface-wave observations:

(1) Dispersion varies with direction of propagation, such as found by Forsyth (1975) for FR and FL across the NAZCA Plate.
(2) Energy (group velocity) propagates along a minimum time path such as a great circle, but the phase velocity deviates from this direction except when there is sagittal symmetry.
(3) The interdependence of the transverse and sagittal components results in apparent coupling of the Rayleigh- and Love-wave trains.

Crampin & Taylor (1971) examined surface wave propagation in an isotropic continental structure with 30 km of aligned crystalline olivine in the upper mantle. Even with this substantial thickness of particularly anisotropic material, surface wave propagation was similar, in many respects, to propagation in purely isotropic structures.

The only characteristics which unambiguously demonstrate anisotropic behaviour are polarization anomalies, particularly the polarization of 3G (corresponding to isotropic 2R). Crampin (1975) examined the effects on polarization of several thicknesses and symmetry orientations of an anisotropic layer. A thickness of as little as 5 km of olivine can result in strong coupling of the transverse and sagittal components of 3G wave trains, but will have very little effect on the equivalent of FR and FL, where such effects might be disguised by, or misinterpreted as, lateral refractions.

Crampin (1975) demonstrated that the polarization at the surface was characteristic of the orientation of the propagation direction to the symmetry planes of the anisotropic layer. It was also shown that anisotropy would have its major effect on the polarization of the 3G mode, the anisotropic equivalent of the isotropic 2R. The particular coupling observed in this paper, an *Inclined Rayleigh* wave where the motion is elliptical in a vertical plane at an

angle to the direction of propagation, is characteristic of anisotropy when there is a horizontal plane of symmetry. This is a likely situation for any anisotropy present in the upper mantle.

5 The effects of anisotropic Earth structures

The characteristics of surface waves have been examined for a number of continental Earth structures containing a layer of anisotropy in the upper mantle, where the anisotropy has a horizontal plane of symmetry. The polarization of the Inclined Rayleigh waves, in particular the second modes, are very sensitive to anisotropy in the upper mantle. This is because the 3G mode in the period band 6–18 s has a large proportion of its energy propagating in the top few kilometres of the upper mantle. We demonstrate these characteristics in diagrams showing the variation with azimuth and period of four quantities describing the motion. These are (1) the dispersion of the phase and group velocity, (2) the inclination of the Inclined Rayleigh motion to the propagation vector, (3) the ratio of the vertical to the horizontal amplitude, and (4) the divergence of the energy propagation from the propagation vector.

These characteristics are shown in Fig. 12 for Model 1 (Table 3), which contains a 10-km thick layer of orthorhombic olivine in the upper mantle of an otherwise isotropic and simplified Earth model. Although orthorhombic olivine is a particularly anisotropic material, the behaviour of the Generalized modes is in most respect very similar to that of isotropic modes, indeed, for propagation in directions of sagittal symmetry in any anisotropic structure, the inclination and group angle are indistinguishable from propagation in isotropic structures. The dispersion curves in Fig. 12 have a velocity variation with azimuth of approximately 2.5, 1.5 and 5.2 per cent for the FG, 2G and 3G modes, respectively, all of which are well within the possible variation in observations of the corresponding isotropic modes caused by small changes in crustal thickness or near surface structure. The ratio of vertical to horizontal motion shows small variation with azimuth, and the maximum divergence of the energy propagation is less than 2°. Similarly, the inclination of the polarization anomaly is very small for the FG, 2G and 4G modes. These departures from isotropic propagation are much less than the anomalies caused by the deviations of Fundamental Rayleigh waves from great circle paths observed by Capon (1970) and Bungum & Capon (1974).

The only distinctive difference from isotropic motion shown in Fig. 12 is the inclination of the 3G mode, which varies up to nearly 60° from the propagation direction, shows wide variation within a small azimuth and period range, and has considerable vertical *and* transverse amplitude for much of its period range. This is qualitatively the type of polarization observed in the polarization diagrams of Figs 4, 6, 8 and 10. Such a varying inclination, together with the variation in the slope of the group velocity dispersion for different azimuths of propagation, which will alter the amplitude and phase of the wave trains at different stations, contributes to the wide variation shown in the observed seismograms of the higher mode wave trains.

Fig. 13 shows the surface-wave characteristics for Model 2, which has an anisotropic layer TIO3070 with a much smaller velocity anisotropy than the olivine layer in Model 1. The transversely isotropic material TIO3070, with horizontal axis, is similar to that fitted by Crampin & Bamford (1977) to Bamford's (1977) observations in western Germany. Fig. 14 shows the velocity variation of plane body waves in the (001)-plane of TIO3070. Despite the 7 per cent *P*-wave velocity anisotropy of TIO3070 being much smaller than the 22 per cent of olivine, the inclination anomalies of 3G in Fig. 13 are very similar in amplitude to

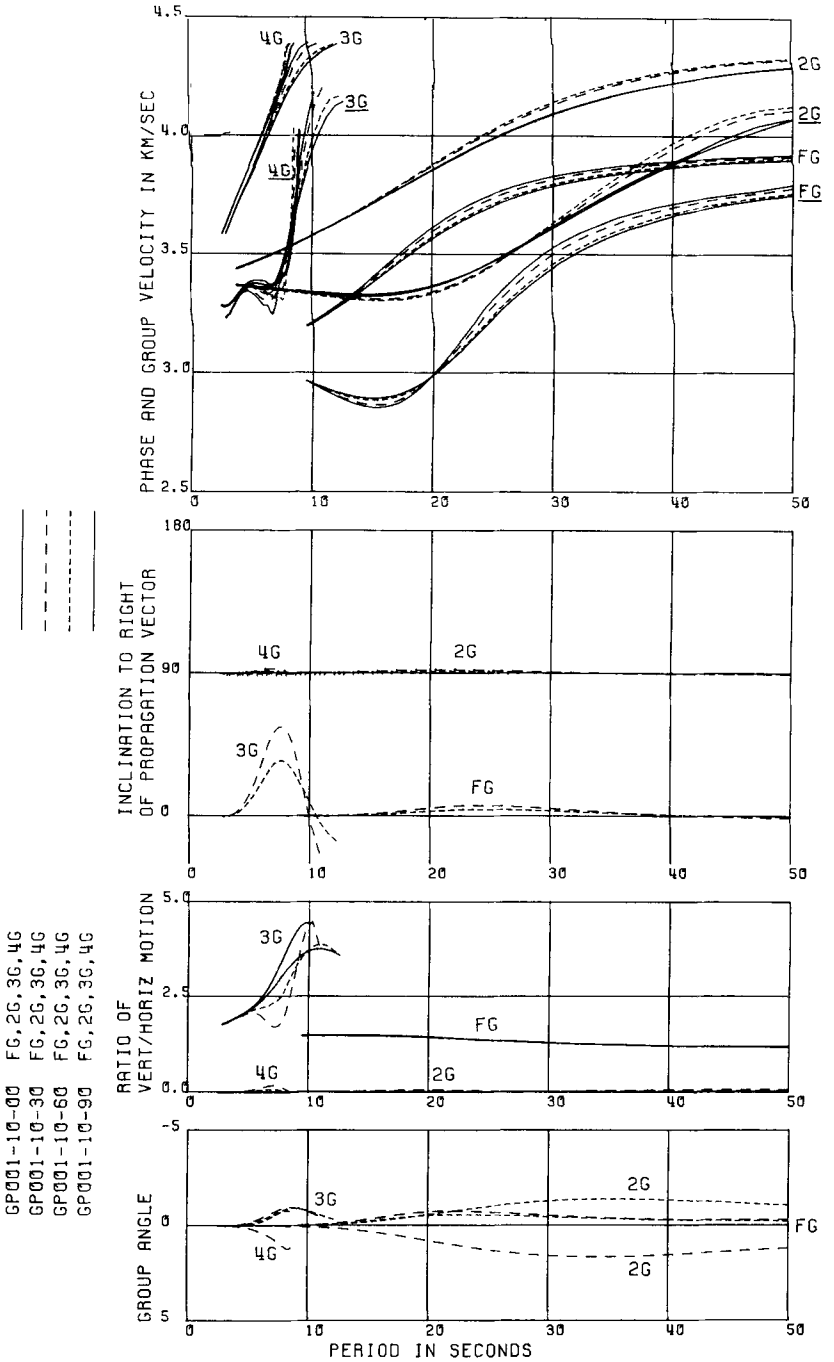

Figure 12. Variation with period of the first four Generalized mode surface waves propagating in four directions (0°, 30°, 60°, and 90° from the 100-direction) in Model 1 (Table 3). The diagrams show (from top): (1) Phase and group velocity dispersion, where the mode identifier of the group velocity is underlined. (2) Inclination (in degrees) of the vertical plane of retrograde elliptical motion to the propagation vector. The prograde motion is hatched. (3) Ratio of vertical amplitude to horizontal amplitude. (4) Divergence (in degrees) of energy propagation to the right of propagation vector.

Note: The group angle is non-zero, except for sagittal symmetry (0° and 90° from the 001-direction), consequently the phase and group velocity dispersion is not coplanar. However, because the group angle is small, this divergence is usually negligible. For propagation in directions of sagittal symmetry the inclination angle is 0° for FG and 3G, and 90° for 2G and 4G, resembling isotropic Rayleigh, and Love waves, respectively.

Table 3. Earth models with anisotropy in the upper mantle.

Identifier	h (km)	ρ (g/cm^3)	α (km/s)	β (km/s)
(1) GP00110	10	2.7	5.8	3.4
	20	2.9	6.6	3.8
	10	3.324	(001)-cut orthorhombic olivine (Verma 1960)	
		3.6	8.1	4.4
(2) BG00110	10	2.7	5.8	3.4
	20	2.9	6.6	3.8
	10	3.324	compound TIO3070 made up of 30 per cent transversely isotropic olivine with horizontal a-axis + 70 per cent isotropy: $\rho = 3.324, \alpha = 7.5, \beta = 4.3$	
		3.6	8.1	4.4
(3) BV00110	10	2.7	5.8	3.4
	20	2.9	6.6	3.8
	10	3.324	TIO3070	
		3.6	9.0	5.2
(4) AJ001x (where x equals 10, 20 or 30 km)	10	2.7	5.8	3.4
	20	2.9	6.6	3.8
	x	3.324	TIO3070	
	40	3.3	7.5	4.3
		3.6	8.3	4.7

those in Fig. 12. Crampin (1977) noted that polarization anomalies in anisotropic media are sometimes almost independent of the degree of anisotropy present. It is a consequence of the completely different character of wave propagation in anisotropic media, where the three propagating plane waves in any given direction, one quasi-longitudinal and two quasi-shear waves, have different velocities, and have particle motion polarizations which are fixed by the orientation of the propagation direction to the elastic symmetry.

The exact behaviour of the 3G inclination depends on the type and orientation of anisotropy in the upper mantle, the thickness of the layer, and on the velocities and thicknesses of the adjacent isotropic layers. The computer programs used to calculate the characteristics are expensive in CPU time, and results are laborious to edit because of problems caused by the small separation of the 3G and 4G modes. Consequently, no systematic numerical examinations have yet been made of the possible effects of different orientations of different anisotropic structures surrounded by different isotropic layers. It is difficult to even place bounds on the possible variations of inclination without extensive numerical investigations. The gross Earth structure is not well determined for shear waves in the upper mantle and the choice of possible anisotropic structures, which are presumably second-order variations on the gross structure, is very wide.

Surface-wave characteristics have been calculated for a limited number of structures. Of these, a range of structures consisting of isotropic crust, anisotropic upper mantle, and isotropic halfspace with no low-velocity zone (no LVZ), produce effects on the inclination very similar to those in Figs 12 and 13. Within this range, the inclination is not critically dependent on the anisotropic symmetry, nor on the degree of velocity anisotropy present.

In the limited number of structures so far examined, there are two classes of structure which produce almost transverse 3G inclinations similar to those observed. Both these classes of structure are possibly rather unrealistic.

The first class of structures which produce almost transverse inclinations for the 3G

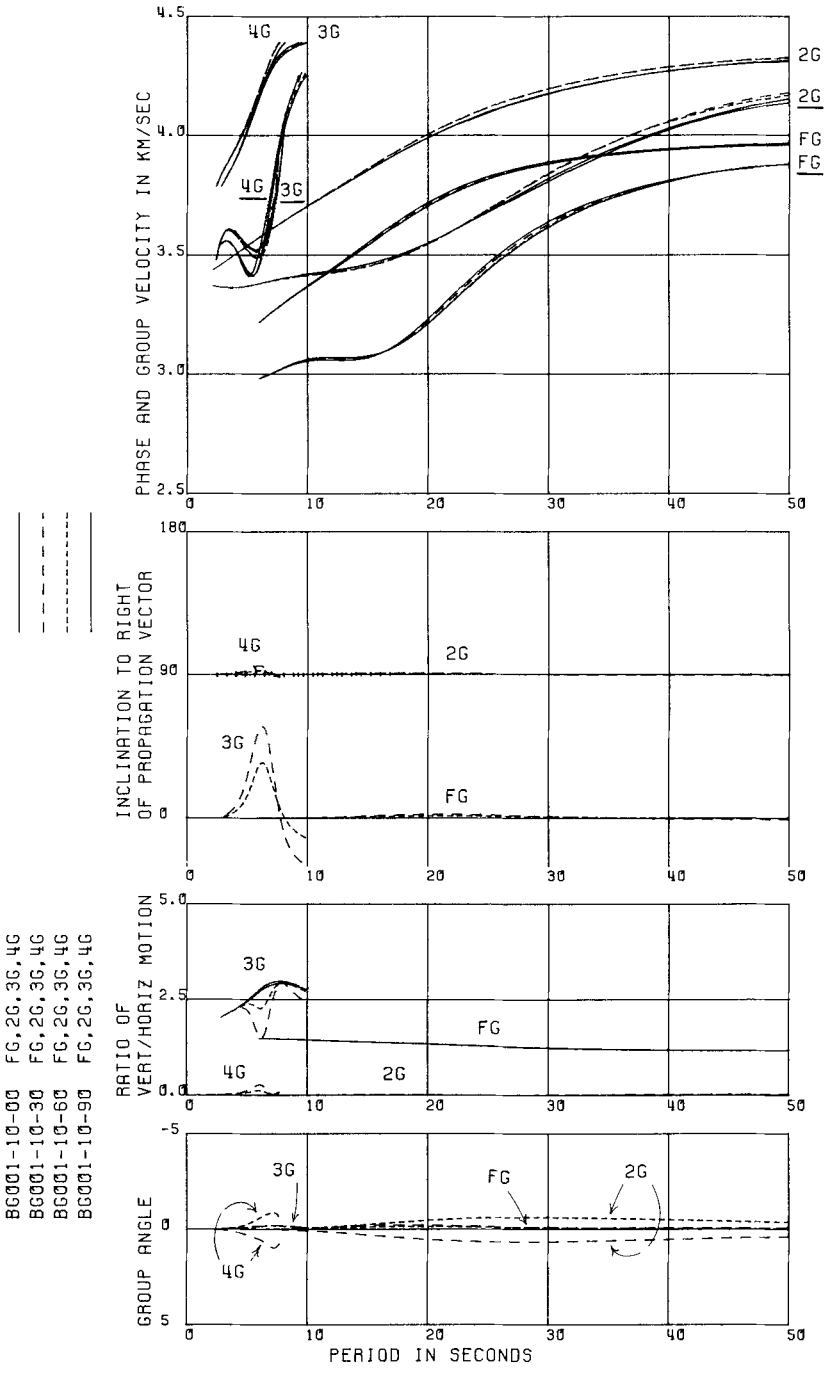

Figure 13. Variation of the first four modes propagating in four directions (0°, 30°, 60°, and 90° from the 100-direction) in Model 2.

modes are those with high-velocity half-spaces. Fig. 15 shows the surface wave characteristics for Model 3, which has 10 km of TIO3070 in the upper mantle over a high-velocity isotropic halfspace. The only distinctive difference from isotropic propagation occurs in the 3G and 4G modes, whose relationship is very complicated where the modes exchange plane

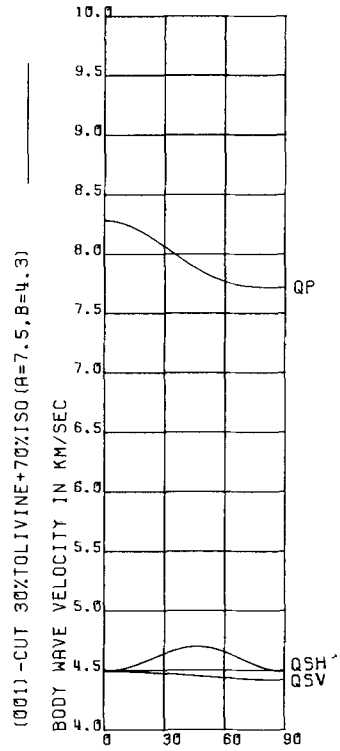

Figure 14. Variation with azimuth (measured from 100) of the quasi-*P*, quasi-*SH*, and quasi-*SV* body waves propagating in the plane of (001)-cut TIO3070.

wave roots at the two places at which the modes pinch together. This results in both modes having transverse polarization with a large vertical component at several places in their dispersion. Another feature of Fig. 15 is the marked difference in the behaviour of 3G and 4G for different directions of propagation. Clearly there is an enormous range of possible 3G and 4G inclination behaviour for different anisotropic structures and different orientations.

Another class of structures which can produce nearly transverse 3G inclinations are those with a LVZ in the upper mantle beneath the anisotropy. Fig. 16, shows the characteristics for Model 4, for a fixed direction of propagation in three different thicknesses of TIO3070 over a 40-km LVZ and an isotropic halfspace. The 3G dispersion curves are disturbed and the transverse inclinations do not occur on the normally dispersed wave train as observed on the seismograms, however, both 3G and 4G show the Inclined Rayleigh motion with polarization nearly perpendicular to the propagation vector.

Fig. 16 also demonstrates another feature of anisotropic surface-wave propagation. Although inclinations of the 3G mode are often very sensitive to variations in structure, there are structures where the inclinations appear to be stable, in that the inclinations remain similar despite substantial changes in the structure. Fig. 16 shows the effects of one such structure, where the inclinations remain basically the same although the thickness of the anisotropic layer varies by 300 per cent. The inclinations illustrated in the polarization diagrams seem to show such stability, where the characteristic pattern appears on wave trains from a large number of paths.

The 3G inclinations in the numerical examples are very sensitive to changes in the parameters of some structures and less sensitive to others. The behaviour of the 3G inclinations is

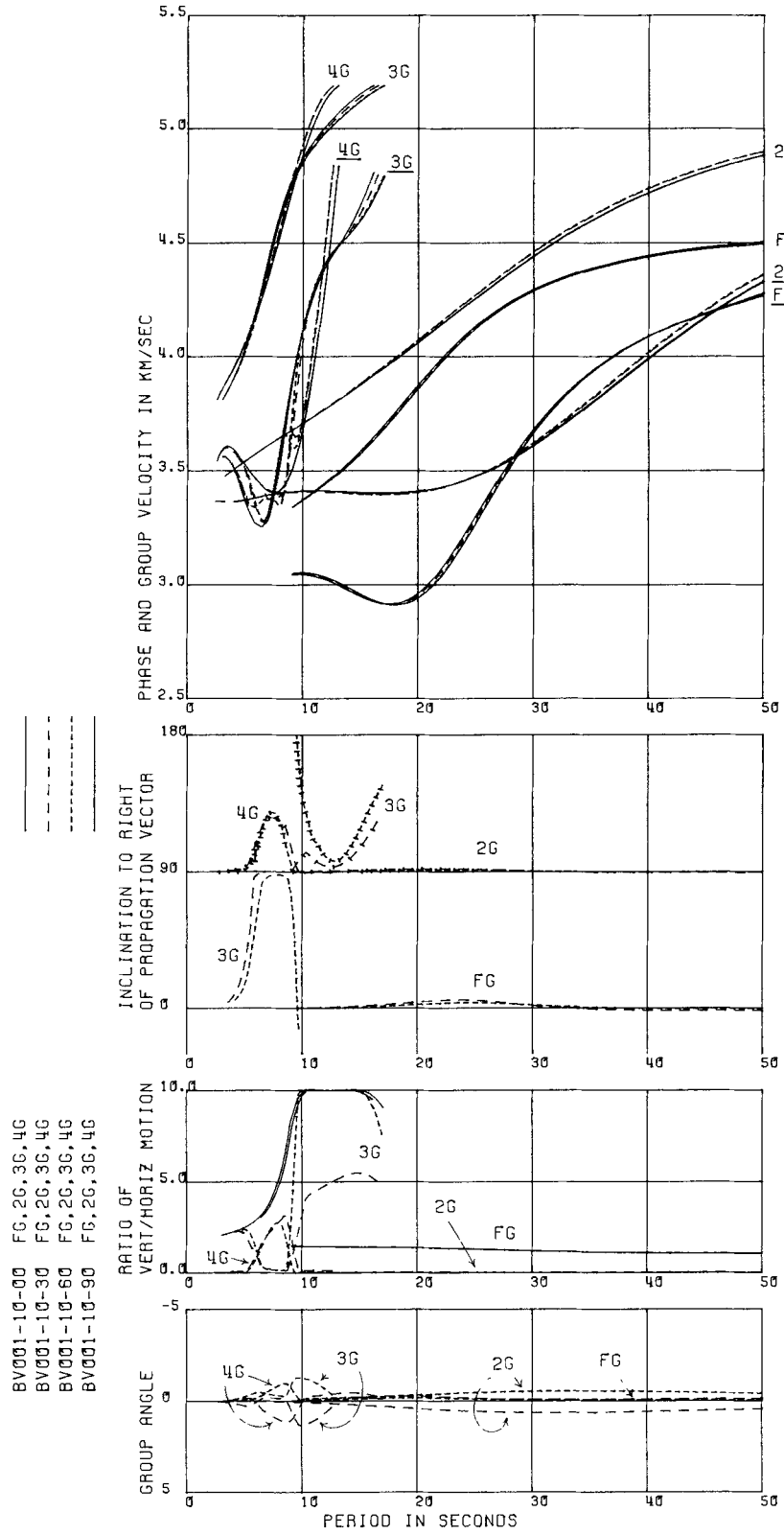

Figure 15. Variation of the first four modes propagating in four directions (0°, 30°, 60°, and 90° from the 100-direction) in Model 3.

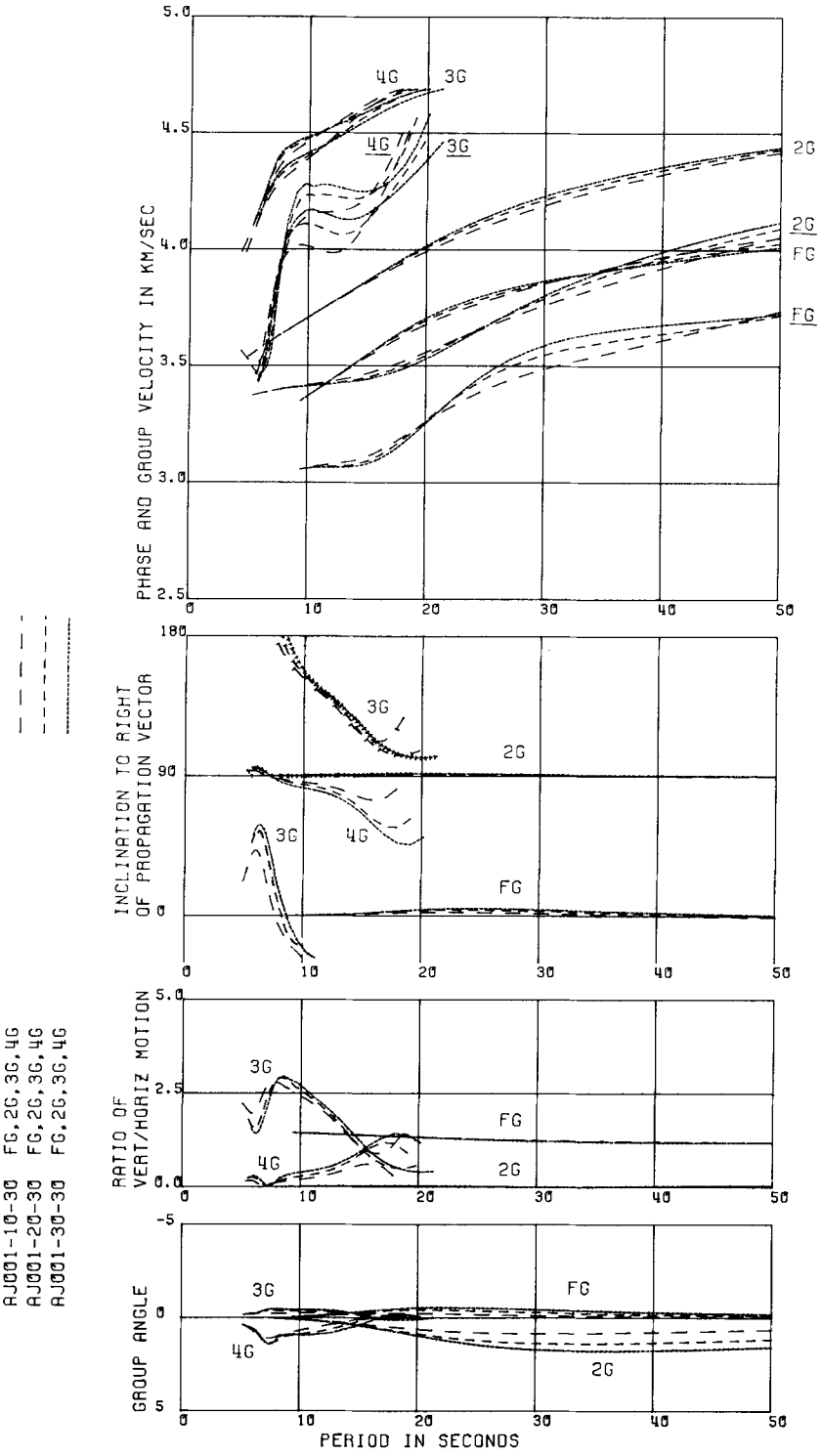

Figure 16. Variation of the first four modes propagating at 30° from the 100-direction in Model 4 with three thicknesses of TIO3070: 10 km, 20 km and 30 km.

a function of the degree of sagittal/transverse coupling in the plane wave decomposition of the surface wave modes. Other coupling phenomena frequently show this type of stable/unstable behaviour: surface wave modes, decoupled by a LVZ in an isotropic model, vary gradually while the LVZ isolates each mode, and at this stage are not very sensitive to small changes of structure. This situation changes at frequencies at which the modes are partially coupled across the LVZ. At such frequencies small changes in structure can radically alter the propagation characteristics. The behaviour of second mode inclinations shows exactly this type of phenomenon, where the modes are now coupled by the polarizations of the quasi-shear waves in the plane-wave decompositions of the surface modes.

Conclusions

The arguments in this paper hang on the recognition that second-mode propagation across Eurasia has anomalous polarization – that is anomalous particle motion. It would be a fair comment to say that particle motion is generally held in low repute by seismologists, and indeed it is difficult to analyse; requiring digital or digitized three-component records, and being very sensitive to local irregularities of structure. It is also difficult to find a suitable technique to display the polarization in a sufficiently concise and comprehensible manner. Certainly the polarization diagrams used here are expensive of space and are tedious to examine. However, the recognition elsewhere that P_n anisotropy exits in the upper mantle, and the demonstration (for surface waves in this paper, and for body waves in Keith & Crampin 1977) that even considerable amounts of anisotropic material in the upper mantle produce only subtle differences from purely isotropic propagation, except for the polarization anomalies, suggests that polarization studies are an important technique for examining Earth structure. It is the need to demonstrate the implications of polarization that provides the justification for the somewhat large number of seismograms presented in this paper.

The sensitivity of polarization to the presence of anisotropy means that the particle motion of body and surface show many anomalies which would have been previously inexplicable in terms of an isotropic Earth.

We have been unable to find a model structure which reproduces quantitatively the polarization anomalies which have been observed in the second-mode wave trains. At the present stage in this investigation, structural models are tested on a trial and error basis, where the greatest problem has been to define a set of anisotropic structures which are geophysically probable or possible. Nevertheless, the examples presented here indicate the very wide range of inclination/structural interactions. When the range of possible anisotropic structures can be outlined in more detail, the higher mode inclinations presented here will have great potential as a structural discriminant.

This paper presents evidence suggesting that a large part of the Eurasian upper mantle (and by implication all continental upper mantles) is anisotropic and that as little as 10 km of a material possessing 7 per cent velocity anisotropy is probably sufficient to produce the observed surface-wave polarizations. No upper limit can yet be placed on the thickness of the anisotropy, and it should be noted that even a substantial thickness of material with *P*-wave velocity anisotropy in the upper mantle would result in only small variations to many seismic observations. The passage of a *P* wave through a 100-km layer of 7 per cent anisotropy in the upper mantle would produce an azimuthal variation of up to 1 s in teleseismic arrival time, which is well within the expected accuracy of general travel-times tables. It appears that observations of an anisotropic Earth, made with low resolution, can be adequately modelled by an isotropic Earth (except for polarization anomalies). However, Crampin (1976, 1977) has demonstrated that, if anything more than a very thin layer of

anisotropy exists in the upper mantle, high resolution observations cannot be approximated by isotropic models. Consequently, if anisotropy exists, almost every calculation of body and surface waves, which sample the upper mantle, must be modified to take account of the presence of anisotropy, if the measurements are made with sufficient resolution. We may phrase this in another way: the resolving power of any direct or indirect inversion of seismic data using isotropic models is limited by the effects of anisotropy in the upper mantle on the observations.

Acknowledgments

The authors wish to thank Dr E. S. Husebye for making available to them the facilities at NORSAR. The Soviet microfilms were obtained by courtesy of Mme Professor N. V. Kondorskaya and World Data Centre B.

The work undertaken by SC was part of the research programme of the Institute of Geological Sciences and is published with the approval of the Director, IGS.

References

Bamford, D., 1977. P_n velocity anisotropy in a continental upper mantle, *Geophys. J. R. astr. Soc.*, **49**, 29–48.

Bungum, H. & Capon, J., 1974. Coda pattern and multipath propagation of Rayleigh-waves at NORSAR, *Phys. Earth planet. Int.*, **9**, 111–127.

Burton, P. W. & Blamey, C., 1972. A computer program to determine the spectrum and a dispersion characteristic of a transient signal, *HMSO AWRE Report 0-48/72.*

Capon, J., 1969. High-resolution frequency-wave number spectrum analysis, *Proc. IEEE*, **57**, 1408–1418.

Capon, J., 1970. Analysis of Rayleigh-wave multipath propagation at Lasa, *Bull. seism. Soc. Am.*, **60**, 1701–1731.

Crampin, S., 1964a. Higher modes of seismic surface waves: preliminary observations, *Geophys. J. R. astr. Soc.*, **9**, 35–57.

Crampin, S., 1964b. Higher modes of seismic surface waves: phase velocities across Scandinavia, *J. geophys. Res.*, **69**, 4801–4811.

Crampin, S., 1966a. Higher modes of seismic surface waves: propagation in Eurasia, *Bull. seism. Soc. Am.*, **56**, 1227–1239.

Crampin, S., 1966b. Higher-mode seismic surface waves from atmospheric nuclear explosions over Novaya Zemlya, *J. geophys. Res.*, **71**, 2951–2958.

Crampin, S., 1967. Coupled Rayleigh-Love second modes, *Geophys. J. R. astr. Soc.*, **12**, 229–235.

Crampin, S., 1970. The dispersion of surface waves in multilayered anisotropic media, *Geophys. J. R. astr. Soc.*, **21**, 387–402.

Crampin, S., 1975. Distinctive particle motion of surface waves as a diagnostic of anisotropic layering, *Geophys. J. R. astr. Soc.*, **40**, 177–186.

Crampin, S., 1976. A comment on 'The early structural evolution and anisotropy of the oceanic upper mantle', *Geophys. J. R. astr. Soc.*, **46**, 193–197.

Crampin, S., 1977. A review of the effects on anisotropic layering on the propagation of seismic waves, *Geophys. J. R. astr. Soc.*, **49**, 9–27.

Crampin, S. & Bamford, D., 1977. Inversion of *P*-wave velocity anisotropy, *Geophys. J. R. astr. Soc.*, **49**, 123–132.

Crampin, S. & Taylor, D. B., 1971. The propagation of surface waves in anisotropic media, *Geophys. J. R. astr. Soc.*, **25**, 71–87.

Dziewonski, A., Bloch, S. & Landisman, M., 1969. A technique for the analysis of transient seismic signals, *Bull. seism. Soc. Am.*, **59**, 427–444.

Forsyth, D. W., 1975. The early structural evolution and anisotropy of the oceanic upper mantle, *Geophys. J. R. astr. Soc.*, **43**, 103–162.

Keith, C. M. & Crampin, S., 1977. Seismic body waves in anisotropic media: synthetic seismograms, *Geophys. J. R. astr. Soc.*, **49**, 225–243.

Mack, H., 1972. Spatial coherence of surface waves, *SACC. Rep. No. 8, Teledyne Geotech.*

Tolstoy, I. & Usdin, E., 1953. Dispersive properties of stratified elastic and liquid media: a ray theory, *Geophys.*, **18**, 844–870.

Verma, R. K., 1960. Elasticity of some high density crystals, *J. geophys. Res.*, **65**, 757–766.